AL-QADISIYAH JOURNAL FOR ENGINEERING SCIENCES 14 (2021) 047–051

Contents lists available at http://qu.edu.iq

Al-Qadisiyah Journal for Engineering Sciences

Journal homepage: https://qjes.qu.edu.iq

The effect of rotational speed on the performance of the electric submersible pump

Hussam Ali Khalaf [a,b,*] **,** ***Wisam Nathem Abd*** [b] **and** ***F. Kh. Tazyukov*** [c]

[a]*Petroleum and Gas Engineering Department, College of Engineering, University of Thi-Qar, Iraq*
[b]*Mechanical Engineering Department, College of Engineering, University of Thi-Qar, Iraq*
[c]*Kazan National Research Technological University, Russia, Kazan*

ARTICLE INFO

Article history:
Received 05 December 2020
Received in revised form 15 January 2021
Accepted 22 February 2021

Keywords:
Rotating speed
Pump performance
Submersible Pump

ABSTRACT

The electric submersible pump (ESP) is a centrifugal pump with several stages. It's a dependable and efficient industrial lifting tool for lifting different amounts of fluids, and it's known for its adaptability and reliability. Electric submersible pumps are commonly used in onshore oil wells, as well as underground pumping and other applications. The pump's efficiency is evaluated under the control of various rotational speeds. The CFD approach is used in this analysis to analyze flow behaviors within the ESP at various flow speeds. ANSYS CFX program was approved to conduct and investigate a single-stage simulation of the GN7000 pump. The sensitivity of the network was determined, and the best mesh for the solution was chosen. The flow field was solved using the (SST, Unsteady-RANS) model with different rotational velocities (2500-3000-3500 cycle in this case). The test used two fluids with varying viscosities, and the findings revealed that the viscosity has an impact on efficiency as well. There is a high level of compatibility as compared to previous studies. This research presented a set of curves for efficiency and pressure and to know the extent of the effect of rotational speed on performance in general.

1. Introduction

Submerged centrifugal pumping is one of the most widely used synthetic lifting technologies in the industry because of its broad applicability in viscous oil flows Thomas et al., [1] The fluid receives energy in the form of pressure, which raises it to the surface in this method of pumping. In a nutshell, ESP is as follows. Power is transferred from the surface (generator) to the induction motor by an electrical cord, where it is converted into mechanical energy. The motor spins the shaft connected to the multi-stage pump, converting mechanical energy to hydraulic energy. The ESP is divided into stages, each of which consists of a rotor that moves and a diffuser that is fixed (stationary). Owing to the strong rotation exerted on it, the rotor provides the fluid's velocity. The fluid is guided to the pump's outlet by the diffuser (or to the next stage of the pump). The rotor and diffuser of the REDA GN7000 style centrifugal pump used in the lift oil are shown in Fig.1. In recent years, a slew of studies aimed at better understanding ESP have been conducted Estevam, [2]; Amaral, [3].

* *Corresponding author.*
E-mail address: hussam.khalaf@utq.edu.iq (Hussam Ali Khalaf)

https://doi.org/10.30772/qjes.v14i1.743

Nomenclature

g	gravity acceleration (m s^{-2})
H	head (m)
$Q_{des,w}$	the volumetric flow rate (m^3/s)
S_{Cor} S_{cf}	the Coriolis and centrifugal effects
P	pressure (pa)
Re_w	rotating Reynolds number
D_h	hydraulic diameter (m)
D_s	the length scale of the pump geometries
U	average peripheral or tangential flow velocity (m s^{-1})
Δp	pressure difference
t	time

Symbols

∂	Derivative
∇	Gradient

Greek symbols

μ	dynamic fluid viscosity kgm^{-1}s^{-1}
ρ	density kg m^{-3}
η	pump efficiency %
ϕ	specific capacity
Γ	generic diffusion coefficient of the general transportation

Subscripts

i	inlet
o	outlet
Z	blade number
D	diameter
b	blade height
e	blade thickness
β	blade angle

With the discovery of new oil fields, several operators have increased their use of this tool along the Brazilian coast. ESP distinguishes itself from other synthetic lifting systems by being the most effective in maritime applications. It is necessary to know the pressure losses present in both the rotor and the diffuser at each point to test the ESP system's efficiency. The efficiency of the pump is determined by the output of each point. Pump output curves are crucial since they describe the pump's efficiency. The impact of various spin speeds on pressure differences, as well as the impact on the efficiency of the electric submersible pump and other factors that cause failure, will be discussed. It is critical to understand each category of failure to assess results. The Hydraulic Institute's pump curves are commonly used in the industry and are a valuable guide for the use of centrifugal pumps. However, since these curves are built with water as the test fluid, they are inadequate as a benchmark for ESP results. In the oil industry, oils from different regions have different properties, and viscosity has a direct impact on pressure losses and velocity in the ESP level, and thus on their efficiency. Several previous experiments on the effects of rotational velocity and viscosity have been conducted, and the findings of these studies have been published. They have studied the effect of speed on performance Yang Y. et al. [4], Zhou L. et al. [5], and studied the effect of viscosity on ESP performance Amaral et al. [6], Gulich J.F [7], Barrios L.J., et al. [8], Paternost G.M. et al. [9], Zhu J. et al. [10], Ofuchi E.M. et al. [11], Patil A. and Morrison G. [12].

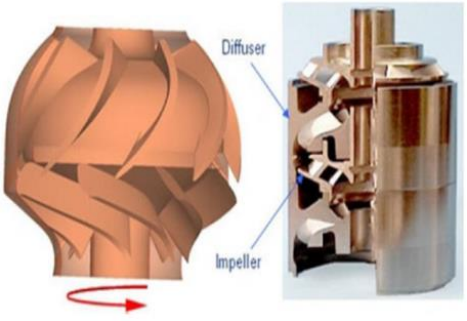

Figure 1. Vane diffuser and Impeller blade, one stage, [3].

The objectives of this work are:

1. A numerical study, network sensitivity test, and validation of the designed model with previous researchers.
2. This work aims to study and determine the losses that occur within a single stage of a centrifugal pump.
3. Knowing the effect of different rotational speeds on the performance of the electric submersible pump using fluids.

2. Numerical methods

2.1. Geometry model and mesh generation

The model was designed by AutoCAD software for the GN7000 pump and simulated by ANSYS20 and generated a network for it. The network used in this study and shown in Fig.2. The whole field group is about 3,010,000 elements. The network is mainly composed of tetrahedral elements and is at the edges of the blades and the subfield interfaces. As well as the hexahedral elements used in the internal field. The sensitivity of the network was tested taking this into account. Take into consideration the following things (Control Body Scaling - Adjust Amplification - Face Tangle Control).

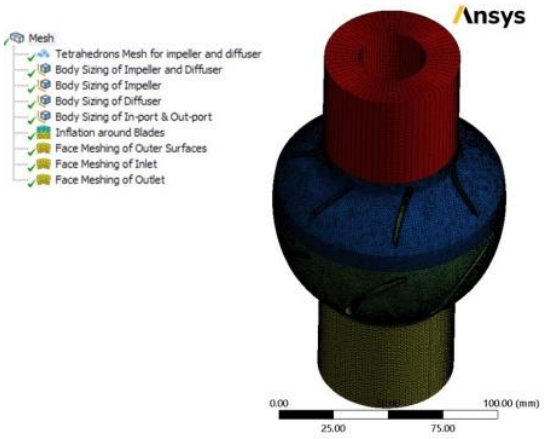

Figure 2. Control processes for mesh generation.

Fig.3 illustrates the control process in grid generation where the operating load is set to flow rate Q = 1 and rotation speed of 3500 rpm to calculate the pressure difference values across the field. Through Fig.3 we notice the greater the number of elements of the network by making improvements, the less the deviation in the pressure difference. Therefore, the closest value

was obtained through the network used in this research in comparison with the research of Stel et al [13] and was adopted in this study.

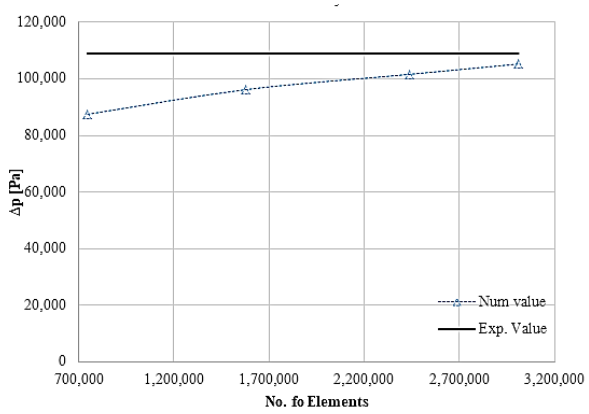

Figure 3. Mesh sensitivity test results; comparison between numerical results and experimental value[3].

2.2. Boundary conditions and main specifications

Fluids have been modeled using ANSYS CFX in a variety of ways, including geometry and grid forms. The fluid analysis problem is solved using pre-treatment based on Navier-Stokes equations. The CFX program can solve unstable governing equations. The mass and momentum equations known as the Reynolds - Averaged Navier - Stokes equations (U-RANS) can be expressed in the following general form:

$$\rho\left(\partial\emptyset/\partial t+\nabla.\left(\vec{V}\emptyset\right)\right)=\nabla.(\Gamma\nabla\emptyset)+S \quad (1)$$

The pump is designed to spin at 3500 rpm (58.33 rev/sec) with n_{des}=3500 rpm. The producer's productivity is at its peak when working with water. It has a volumetric flow rate of $1.360x10^{-2}$, a mass flow rate of 13.6 kg/s, and a head of 9.6 m. Because of the following theorem, the designed volumetric flow rate will change if the impeller's spinning speed changes.;

$$Q_{des,w}=(n/3500)\times1.36\times10^{-2} \quad (2)$$

There are four subdomains in the dominant domain. The in-port domain (the intake), the Rotor domain (the impeller), the Stator domain (the diffuser), and the out-port domain (the discharge port) are the four domains, respectively. The inlet face has a continuous reference pressure, pref = 0 (Pa), with a turbulence slope and flow direction of zero. Facade surfaces are used to link sub-domains together (connecting fixed and rotating areas). Non-slip surfaces are required on all surfaces. A boundary state interface with a given discharge fluid flow rate value is known as the outlet surface.

3. Results and discussion

3.1.Pressure difference

All simulation conditions are summarized in Table (1); and all of these cases are simulated for 2500, 3000, and 3500 rpm. By using MPI parallel calculation with 6 CPU processors with a PC of specifications (Intel Core™ i9 CPU 3.5 GHz 32 GB RAM). The simulations need 33 runs and each run demands approximately 36 hrs.

Table 1. Summary of simulation conditions

Case	Working Fluid	Viscosity (cP)	Density (kg/m3)	Flow rate (kg/s)	Reynolds number
01	Pure Water	1	998.2	3.40	47,674
02	Pure Water	1	998.2	6.80	95,348
03	Pure Water	1	998.2	10.2	143,022
04	Pure Water	1	998.2	13.6	190,696
05	Pure Water	1	998.2	17.0	238,370
06	Pure Water	1	998.2	20.4	286,044
07	Oil	24.98	889	3.02200	1,699.705
08	Oil	24.98	889	6.04500	3,399.410
09	Oil	24.98	889	9.06780	5,099.116
10	Oil	24.98	889	12.0904	6,798.820
11	Oil	24.98	889	15.1130	8,498.520

However, Fig.(4) shows the pressure difference concerning flow rate values for water as a working fluid at three different impeller speeds. It has shown that as the angular velocity of the impeller increases, the pressure difference also increases. This is because as the impeller rotation became faster, the flow behaves as a blockage at the rotor zone. Thus, more flow force needs to penetrate this block of fluid, which leads to increased pressure differences across the pump stage. In addition, in the high flow rate cases, the effect of rotational speed degrades the pressure difference. It was found that the pressure change for the volumetric flow rate of Q/Q_{des} = 1.5 is 44.8141% and 32.0046% for 2500 rpm and 3000 rpm respectively lower than the n=3500 rpm case. And in the case of Q/Q_{des} = 0.5, the pressure difference is 71.9994% and 37.298% for 2500 rpm and 3000 rpm respectively lower than the n=3500 rpm case.

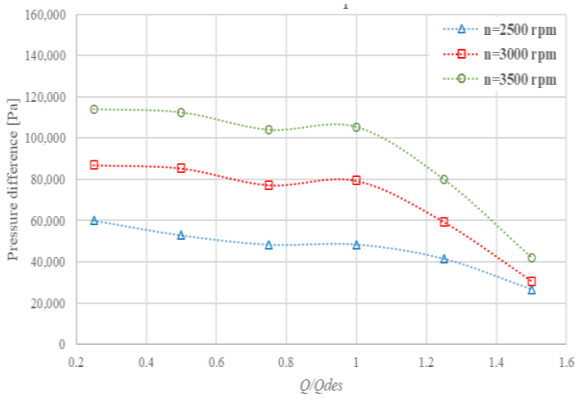

Figure 4. Comparison of pressure difference for water 1cp, at several rotor speeds.

Fig.(5) shows a similar comparison for the 24.98 cP fluid. The same observations were verified by looking at these curves. The pressure difference proportion directly to the angular velocity of the impeller. It's evident from the previous estimates that as the flow rate increases, the velocity of the inlet flow rises with it. This rise in inlet velocity induces more shearing of the fluids and more energy loss. As a result, the pressure differential decreased in situations where the flow rate was higher. Also, in the following figure, it's obvious that for higher fluid viscosity, the pressure rise is lower. It is the same influence of the flow rate increases.

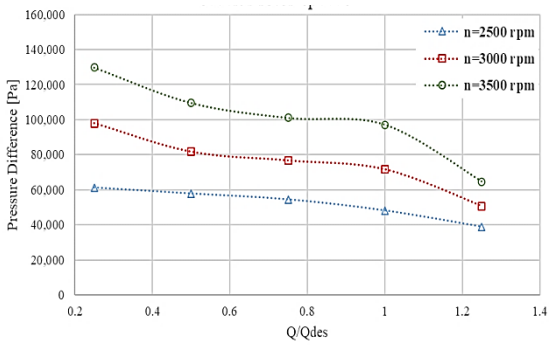

Figure 5. Comparison of pressure difference for oil 24.98 cp, at several rotor speeds.

Also, from the above comparison, it can be observed that the pressure rise is highest in the lowest flow rate condition for each fluid. As the flow rate becomes higher, the pressure difference decreased for fluid with the operating condition or high capacity condition. For the case of $Q/\ Q_{des,w}$ = 1.5 at 3500 rpm, the pressure contour is shown in Fig.(6). The higher-pressure difference appears in the impeller region due to rotational motion. The secondary flow generated leads to high-pressure differences around the blades. Therefore, the pressure difference in the impeller is approximately like the pressure change of the whole stage.

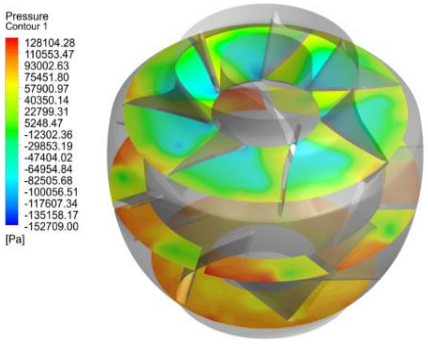

Figure 6. The pressure contour for the case of Q/ Qdes, w = 1.5 at 3500 rpm.

3.2. Analyze the results

To approximate the pump efficiency, the following equation was used:

$$\eta = (\rho\ g\ Q\ H)/T\omega = (Q\ \Delta p)/T\omega \quad (3)$$

Q represents the flow rate (m3/s), H represents the head (m), represents angular speed (rad/s), and T represents the torque (N.m). the torque that can be measured directly from the CFD-post function calculator in the ANCYC CFX program. The XY diagrams for the pump's performance in clear water and another fluid with a viscosity of 24.98 cp for various impeller speeds are published in the following figures. A comparison of two fluids (water and oil) at two different rotational speeds is seen in the diagram below (3000 and 3500 rpm). At the same rotational speed, the highest output point for various viscosity fluids is (3500 rpm). When working with water, Q / Qdes = 1 is the flow rate at the best performance stage. When treating a fluid with a viscosity of 24.98cp, the flow rate drops to Q / Qdes = 0.8 at the best Efficiency stage. When interacting with a lower rotational speed, the same explanation can be seen (3000 rpm). The best performance point has declined, as we can see. We may assume that the rotational speed has a significant impact on efficiency and that the viscosity of the electric submersible pump is affected.

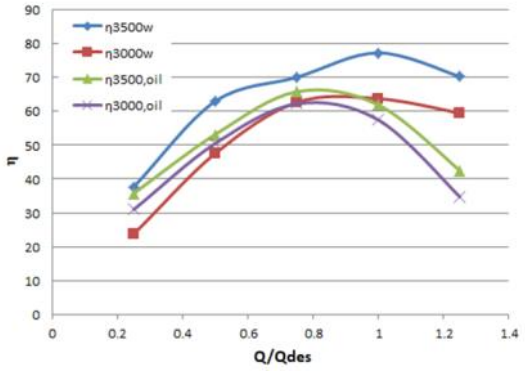

Figure 7. Best efficiency points are different for various rotational speeds and viscosity fluids.

The best performance point shifts from Q/Qdes =0.8 at 3500 rpm to roughly Q/Qdes =0.68 at 2500 rpm, as seen in the graph above. This is because as the rotational speed reduces, so does the angular flow speed. For a constant volumetric flow rate, this resulted in the velocity vector in a diffuser flow not being in the same direction. To achieve the same combination of axial and angular velocity in the diffuser component, the flow rate should be reduced as well. In the diffuser and out-port areas, this mixture resulted in blade-oriented flow. However, in the considered ESP model, the best performance point shift for both water and oil flow.

3.3. Dimensionless analyses

It was determined to do a dimensionless analysis. The dimensionless numbers were used in this analysis to investigate the effect of viscosity on ESP performance. The equations below are used to calculate the dimensionless numbers. The precise capability;

$$\Phi = \frac{Q}{\omega D_s^3} \quad (4)$$

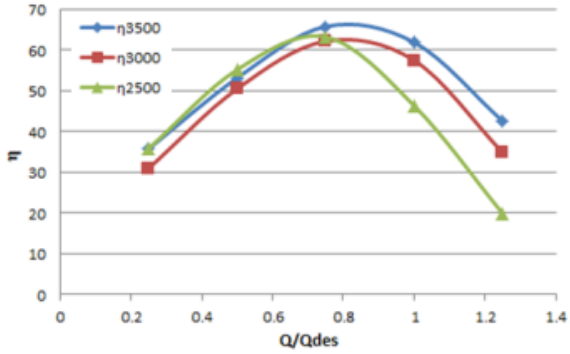

Figure 8. Efficiencies for three rotational speeds are explained in the XY plot for oil flow.

Using Q as the stage's flow rate (m3/s), $\omega$is the impeller's angular speed (rad/s), and Ds is the impeller outlet mean diameter, which is the average of the inner and outer diameters. The value of Ds in this model is 0.0884 m. There's also the spinning Reynolds number to consider.

$$Re_w = \frac{\rho \omega D_s^2}{\mu} \quad (5)$$

where ρ is the operating fluid's density (kg/m3) and μ is the fluid's mechanics viscosity (kg/m.s). The rotating Reynolds numbers for all simulation cases are described in Table (2). The rotational Reynolds number gives the same impression as the traditional Reynolds number.

Table.2. Rotating Reynolds numbers for all simulated cases.

Water			Oil		
n=2500	n=3000	n=3500	n=2500	n=3000	n=3500
2042161.47	2450597.4	2859030.3	72808.459	87370.2803	101931.994

The increasing velocity (in this case angular velocity) led to increasing Re_w. The increase of viscosity results to reducing of Re_w value. However, Fig.(9) shows the efficiency versus specific capacity. It has been shown that increasing the revolving Reynolds number increased pump efficiency. Points calculated from simulation data. Using Microsoft Excel, the curves were applied using a polynomial of the fourth-order trend. These performance curves have a starting point that is roughly at the origin. Based on the figure, the efficiency of ESP is a function of the specific capacity and the rotating Reynolds number.

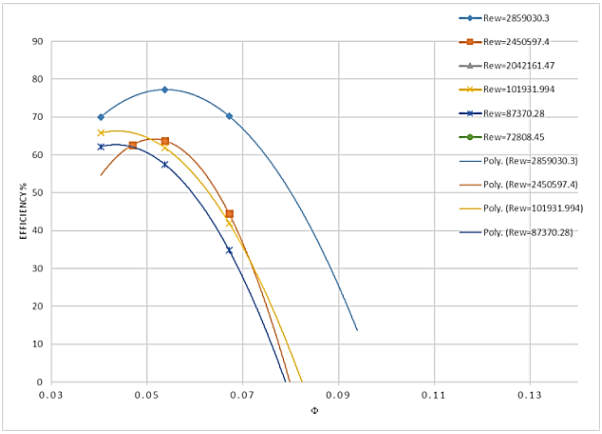

Figure 9. Efficiency versus specific capacity.

4. Conclusion

This paper presents a numerical study of the GN7000 ESP pump that was designed and tested under different rotational velocities and flow rates to create specific operating conditions.

The conclusion includes the following aspects:

1. The arithmetic field was created for one stage with a high-quality structural network, and the sensitivity of the network was analyzed to determine the appropriate network and it was good when compared with previous research.
2. The results showed that the pressure difference concerning the values of the fluid flow rate working at three different impeller speeds, that with increasing the rotational speed, the pressure difference increases.
3. In high-flow rate situations, the effect of rotational velocity on the pressure difference decreases.
4. When comparing the rotational speed (3500-3000-2500 rpm), it was found that the best performance point for different viscous fluids with the same rotation speed is 3500 rpm.

Authors' contribution

All authors contributed equally to the preparation of this article.

Declaration of competing interest

The authors declare no conflicts of interest.

Funding source

This study didn't receive any specific funds

REFERENCES

[1] J. E. Thomas, A. Triggia, C.A. Correia, C.V. Filho, J.A.D. Xavier, J.C.V . Machado, J.E. Filho, J.L. Paula, N.C.M. Rossi, N.E.S. Pitombo, P.C.V. Gouveia, R. Carvalho, R.V. Baragan, Fundamentals of petroleum engineering. Second edition. Rio de Janeiro: Editora Interciência, 2001.

[2] V. Estevam, A phenomenological analysis of the centrifugal pump operation with the two-phase flow, Ph.D. thesis, Faculty of Mechanical Engineering, State University of Campinas, Campinas, 2002.

[3] G.D.L.do Amaral, Modeling of Single-Phase Flow in Submerged Centrifugal Pump Operating with Viscous Fluids, MSc thesis, Faculty of Mechanical Engineering, State University of Campinas, Campinas, 2007.

[4] Yang Yang, Ling Zhou, Weidong Shi, Chuan Wang, Wei Li, Ramesh Agarwal, Effect of Rotating Speed on Performance of Electrical Submersible Pump, ASME-JSME-KSME 2019 8th Joint Fluids Engineering Conference ISBN: 978-0-7918-5905-6, 2019.

[5] Ling Zhou, Wanhong Wang, Jianwei Hang, Weidong Shi, Hao Yan, Yong Zhu, Numerical Investigation of a High-Speed Electrical Submersible Pump with Different End Clearances, Water 2020, 12(4) (2020) 1116; https://doi.org/10.3390/w12041116

[6] G. Amaral, V. Estevam, F.A. Franca, On the Influence of Viscosity on ESP Performance. SPE Production and Operations, 24(02) (2009) 303-311.

[7] J.F. Gülich, Pumping Highly Viscous Fluids with Centrifugal Pumps - Part 2. World Pumps, 396 (1999) 39-42.

[8] L.J. Barrios, S.L. Scott, R. Rivera, K.K. Sheth, ESP technology maturation: subsea boosting system with high GOR and viscous fluid. In SPE Annual Technical Conference and Exhibition. Society of Petroleum Engineers. SPE-159186-MS, 2012.

[9] G.M. Paternost, A.C. Bannwart, V. Estevam, Experimental study of a centrifugal pump handling viscous fluid and two-phase flow, SPE Production and Operations, 30 (02) (2015) 146–155.

[10] J. Zhu, H. Banjar, Z. Xia, H. Zhang, H-Q. Zhang, CFD simulation and experimental study of oil viscosity effect on multi-stage electrical submersible pump (ESP) performance. Journal of Petroleum Science and Engineering, 146 (2016) 735-745.

[11] E.M. Ofuchi, H. Stel, T.S. Vieira, F.J. Ponce, S. Chiva, R.E.M. Morales, Study of the effect of viscosity on the head and flow rate degradation in different multistage electric submersible pumps using dimensional analysis, Journal of Petroleum Science and Engineering, 156 (2017) 442–450.

[12] A. Patil, G. Morrison, Affinity law modified to predict the pump head performance for different viscosities using the Morrison number. ASME Journal of Fluids Engineering, 141 (2) (2019) 021203.

[13] H. Stel, T Sirino, F.J. Ponce, S. Chiva, R.E.M. Morales, Numerical investigation of the flow in a multi-stage electric submersible pump. Journal of Petroleum Science and Engineering, 136 (2015) 41-54.